BIOCHEMISTRY
including biophysical chemistry & molecular biology

ARTICLE

pubs.acs.org/biochemistry

A QM/QM Investigation of the hUNG2 Reaction Surface: The Untold Tale of a Catalytic Residue

Jennifer L. Przybylski and Stacey D. Wetmore*

Department of Chemistry and Biochemistry, University of Lethbridge, 4401 University Drive, Lethbridge, Alberta T1K 3M4, Canada

Supporting Information

ABSTRACT: Human uracil−DNA glycosylase (hUNG2) is a base excision repair enzyme that removes the damaged base uracil from DNA through hydrolytic deglycosylation of the nucleotide. In the present study, the mechanism of hUNG2 is thoroughly investigated using ONIOM(MPWB1K/6-31G(d):PM3) active-site models to generate reaction potential energy surfaces. Active-site models that differ in the hydrogen-bonding arrangement of the nucleophilic water molecule and/or protonation state of His148 are considered. The large barrier calculated using the model with a cationic His148 verifies that this residue is neutral in the early stages of the reaction. The reaction pathways predicted by two models with a neutral His148 are consistent with a wealth of experimental data on the enzyme, including mutational studies, which supports our approach. On the basis of our calculations, we propose a complete mechanism for the chemical step of hUNG2. In the first part of the reaction, His268, Asn204, and a water molecule work together to stabilize the negative charge forming on the uracil moiety. Subsequently, either Asp145 or His148 can act as the general base that activates the water nucleophile depending on the binding orientation of the water molecule in the active site. However, we propose that His148 preferentially acts as the general base. Therefore, in agreement with previous proposals, we assign the primary function of Asp145 to electrostatic stabilization of the positive charge developing on the sugar moiety during the reaction, which is also consistent with a growing theory that the primary function of active-site carboxylate groups present in many glycosylases is transition state stabilization. Most importantly, our work explains, for the first time, the role of His148 in the chemical step and provides additional support for the inclusion of this amino acid in the list of residues (Asp145 and His268) essential to the chemical step of the hUNG2 mechanism.

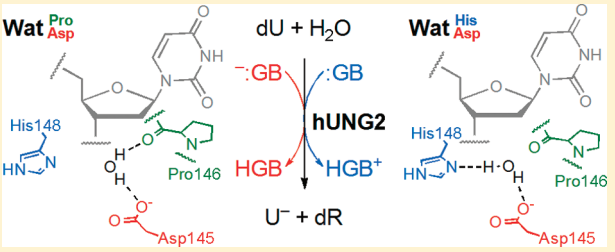

Human uracil−DNA glycosylase (hUNG2) and the *Escherichia coli* homologue (eUDG) have been extensively studied in the literature since their discovery decades ago.[1,2] hUNG2 catalyzes the hydrolysis of the *N*-glycosidic bond in 2′-deoxyuridine, a common form of DNA damage, in single- and double-stranded DNA.[3] There are two main steps involved in the catalytic deglycosylation mechanism: (1) flipping the damaged nucleotide out of the helix and into the active site and (2) hydrolysis of the glycosidic bond through a general base mechanism.[4−6] Because of the high similarity between their sequences and activities, hUNG2 and eUDG have been used interchangeably to investigate the second (chemical) step in a broad variety of experiments, including Raman spectroscopy,[7] kinetic isotope effects,[8] X-ray crystallography,[9−14] NMR spectroscopy,[15−18] and mutational analysis,[10,11,15,19−21] as well as computational studies.[22−25]

On the basis of previous investigations, a stepwise dissociative pathway for the chemical step has been proposed.[4−6,26] In the first (rate-limiting) step of the proposed mechanism (Scheme 1), uracil departs from the DNA backbone to form a uracilate anion. The glycosidic bond cleavage is believed to be catalyzed by a short, strong hydrogen bond between neutral His268[a] and the uracil moiety, while the resulting highly unstable oxacarbenium cation is most likely electrostatically stabilized by the uracilate anion and Asp145 as well as nearby phosphate groups. In the second step of the proposed mechanism, a nucleophilic water molecule irreversibly adds to the anomeric sugar carbon to form an apyrimidinic site (AP-site). During this step, the nucleophile must be activated by proton transfer to a general base,[27] a role assigned to Asp145.

Building on the essential involvement of His268 and Asp145 in the mechanism of hUNG2 action, a recent study by Parker and Stivers uncovered another important active-site residue, namely His148.[18] In addition to contributing to the nucleotide-flipping step,[18,28] it was revealed that His148 makes an important catalytic contribution late in the reaction. The study by Parker and Stivers also shows that His148 is neutral in the unbound protein and at the start of the reaction but becomes protonated as the reaction proceeds. Furthermore, mutation of this residue to alanine decreases binding of TS mimics, which suggests that His148 provides transition state stabilization. On the basis of these results, it was proposed that His148 plays a role in the chemical step, possibly through orienting the nucleophilic water molecule and/or enhancing electrostatic stabilization by

Received: March 7, 2011
Revised: April 6, 2011
Published: April 07, 2011

ACS Publications © 2011 American Chemical Society

Scheme 1

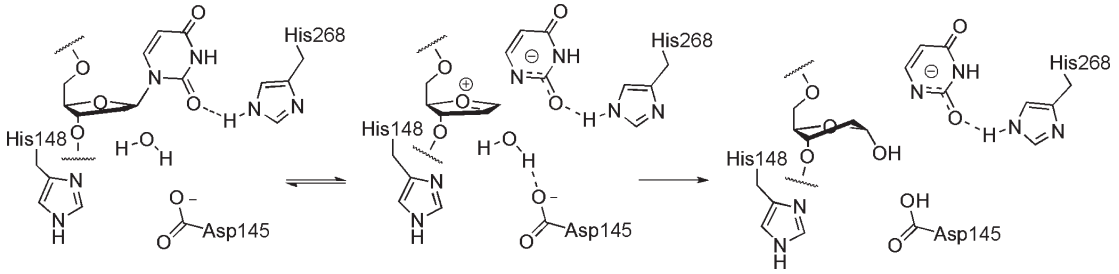

excluding solvent from the active site.[18] Interestingly, this absolutely conserved histidine is within hydrogen-bonding distance of the nucleophile[13,14] and likely has an increased proton affinity due to interactions with a nearby phosphate group. Therefore, it is possible that the role of His148 in the chemical step of the hUNG2 mechanism is to activate the water nucleophile.

It is commonly believed that the general base in the hUNG2 mechanism is Asp145 since mutation of this residue effectively removes the catalytic activity of the enzyme.[10] Independent of this role, it is accepted that Asp145 provides significant electrostatic stabilization to the dissociative transition state and oxacarbenium-cation intermediate.[20,26] Consequently, it is highly plausible that removing this residue prevents catalysis by destabilizing nucleobase departure rather than water activation. Indeed, bifunctional glycosylases (such as hOGG1, FPG, EndoIII, and NEIL1) that do not use a water nucleophile contain an essential carboxylate group (aspartate or glutamate residue) in a similar location with respect to the sugar moiety, and the primary role of this residue is electrostatic stabilization.[29−32] An essential carboxylate group with an electrostatic stabilization role is also found in a comparable location in other monofunctional glycosylases (such as MutY, AlkA, and AAG).[33−35] Interestingly, there are two carboxylate groups in the MutY active site, where one is proposed to stabilize the sugar moiety and the other has been implicated in water activation.[34] Therefore, another residue may be responsible for water activation in hUNG2 without contradicting the key experimental findings regarding the importance of Asp145.

The above discussion suggests that the role of both His148 and Asp145 in the mechanism of hUNG2 action may not yet be fully revealed. Molecular modeling is a useful way to further investigate how these residues are involved in the chemical step of the reaction. Among the computational investigations of hUNG2 to date,[22−25] the most in-depth used QM/MM techniques to model the reaction.[23] A detailed reaction potential energy surface (PES) was generated, primarily to investigate the dissociation step of the hUNG2 mechanism. However, this study was carried out before the initial protonation state of His148 was elucidated,[18] and consequently this residue was modeled as cationic throughout the entire reaction. Furthermore, since His148 was treated at the low (MM) level of theory and the nucleophilic water at the high (QM) level of theory, interactions between these moieties were not accurately described in part because neither charge nor atom transfer can occur across a QM/MM boundary. Finally, only one avenue for water activation was considered, which utilized Asp145. In addition to addressing these technical issues, a more thorough computational investigation of the hUNG2 reaction surface is required to account for, and explain, new experimental evidence that has identified the importance of His148 in the chemical step.

In the current study, the mechanism of hUNG2 action is investigated with a QM/QM active-site model. Detailed reaction potential energy surfaces for several models differing in the nucleophile hydrogen-bonding pattern are used to consider how the enzyme catalyzes uracil dissociation and activates the water nucleophile. Particular attention is placed on the roles of essential active-site residues including the involvement of His268 in base departure and, more importantly, the currently unclear function of Asp145 and His148 in nucleophile activation. In addition, the effect of the protonation state of His148 on the reaction is studied for comparison to previous computational work,[23] and mutational analysis is used to calculate contributions of individual residues to the activation energy. Our extensive calculations allow us to examine the interdependence of the dissociation of the nucleobase and association of the nucleophile during the mechanism and clarify the function of important active-site residues. Through this work, we propose a modified mechanism of hUNG2 action that is consistent with experimental research, clarifies the identity and role of essential active-site amino acids, and supports a unified primary purpose for active-site carboxylate groups present in many (monofunctional and bifunctional) glycosylases.

COMPUTATIONAL DETAILS

Model Generation. The initial geometry for all systems studied was taken from a crystal structure (PDB ID: 1EMH) of human uracil−DNA glycosylase (hUNG2) bound to a reactant mimic (pseudouridine, ψU).[13] First, a truncated model of the hUNG2 active site was generated that contained residues within 10 Å of the ψU glycosidic bond, including 18 discrete water molecules. Within this model, the full ψU nucleotide (P2U5) was included as well as the dT4 and dA6 nucleotides. The phosphate group of the dT7 nucleotide was also included due to its proximity to the reaction center. Subsequently, components of our model that are directed away from the reaction center were truncated because they are not believed to play a role in the chemical step. Specifically, several residues (Table S1, Supporting Information) were modeled as glycine (i.e., only the backbone was included). Additionally, since most of the Ile173 side chain is within 10 Å of the reaction center, the backbone was truncated between C_α and C_β of the residue. Finally, the nucleobases in the nearby nucleotides were modeled as amino groups. Hydrogen atoms were added to the resulting model by inspection, where Asp145 was modeled as anionic and all other residues as neutral. The total charge of the system is −5.

The ONIOM(MPWB1K/6-31G(d):PM3) methodology[36−38] was used on our model system, which treats the low-level region with the PM3 semiempirical method[39,40] and the high-level

dx.doi.org/10.1021/bi2003394 |Biochemistry 2011, 50, 4218–4227

Scheme 2

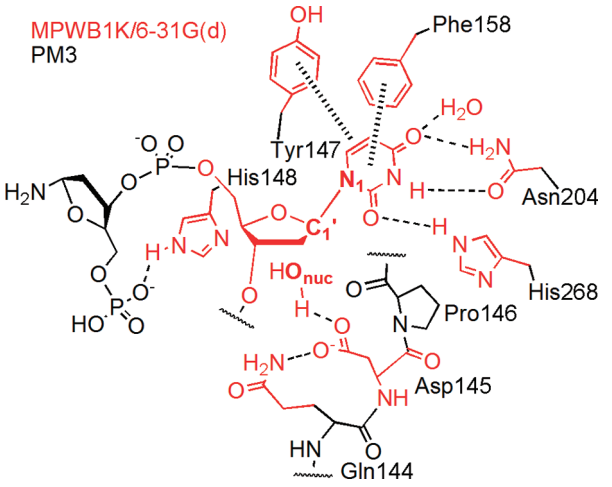

region with the MPWB1K density functional method[41] in conjunction with the 6-31G(d) basis set. The DFT region contains the 2′-deoxyuridine nucleoside, the water nucleophile (W600), an additional water molecule (W727), the full Asp145 residue, and the R-groups of Gln144, Tyr147, His148, Phe158, Asn204, and His268 (Scheme 2). Thus, there are 63 heavy atoms in the DFT region and 248 heavy atoms in the semiempirical region. A detailed description of all groups included in the high and low levels is provided in the Supporting Information (Table S1). Reactant geometries were obtained by initially relaxing all protons at the PM3 level of theory and subsequently relaxing the DFT region using the full ONIOM(MPWB1K/6-31G(d):PM3) method combination. Throughout the remainder of the study, the DFT region was free to optimize, while the semiempirical region was held fixed to this original reactant geometry. The coordinates of the semiempirical region were fixed since overlays of crystal structures of hUNG2 bound to reactant,[13] intermediate,[14] and product[12,13] mimics are substantially similar for all residues included in the low-level region. Finally, the reactant mimic was mutated to uracil, and the DFT region was reoptimized.

Surface Generation. Reaction potential energy surfaces (PES) were obtained by constraining the glycosidic (C1′−N1) and nucleophilic (C1′−O_{nuc}) distances (Scheme 2). One coordinate was systematically altered by an increment of 0.200 Å, and the remainder of the DFT region was allowed to relax. This process was repeated until a stationary point was clearly identified or the change in energy between two points was greater than 40 kJ mol^{-1}. For example, the highly compressed region with glycosidic and nucleophilic distances less than 1.8 Å was not investigated. The (ONIOM(MPWB1K/6-31G(d):PM3)) relative energies (with respect to the corresponding reactant complex) are presented as PES plots for each model (Figure 1), where the reactant well occurs on the left and the product well on the right.

Refinement of Stationary Points. The geometries of the reactant, transition state, and product complexes identified from the PES of feasible reaction pathways were further relaxed. Specifically, the constraints to the reaction coordinates for the reactant and product complexes were removed, and the system was optimized to a minimum with the ONIOM(MPWB1K/6-31G(d):PM3) level of theory. The transition state structure was refined using the quadratic synchronous transit (QST) method,

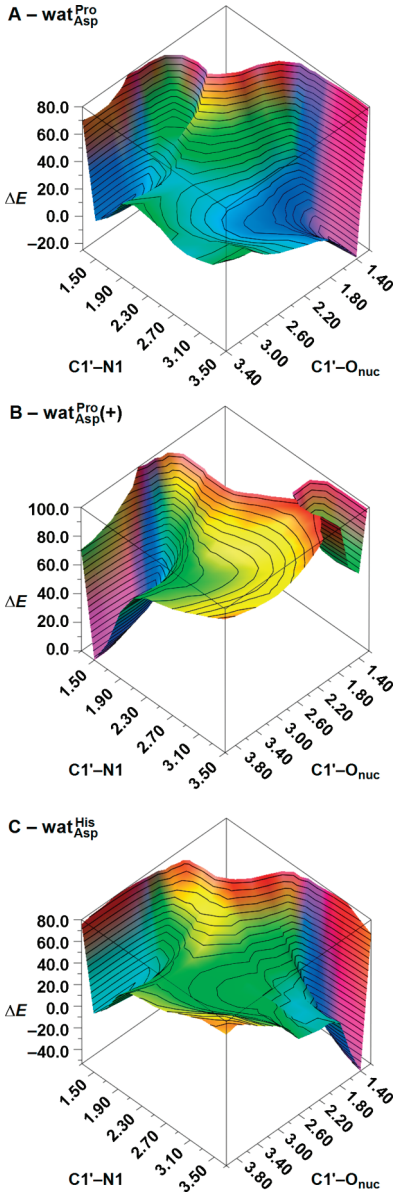

Figure 1. ONIOM(MPWB1K/6-31G(d):PM3) reaction surfaces for the mechanism of hUNG2 action using the wat$^{Pro}_{Asp}$ model (A), the wat$^{Pro}_{Asp}$(+) model (B), and the wat$^{His}_{Asp}$ model (C). The energies (Δ*E*, kJ mol^{-1}) are reported relative to the respective reactant.

with the three complexes from the PES as input. The QST methodology has recently been found to be effective for large models of other biological systems.[42−45] The optimization was considered complete when the forces converged to default criteria and the displacement converged to loose criteria (<0.002 au). Because of computational resource limitations, frequency calculations could not be run on the entire system. Therefore, as in a previous study,[46] the character of the fully optimized stationary points was verified by visual inspection of the normal modes of the high-level region of a system with any atom further than 4 Å from a DFT heavy atom removed. Through this analysis, we find that our fully optimized transition states contain a large imaginary frequency (190−240 cm^{-1}) corresponding to motion along the desired reaction coordinate. Since zero-point energy corrections could not be calculated, the reported relative energies are

dx.doi.org/10.1021/bi2003394 |*Biochemistry* 2011, 50, 4218–4227

Scheme 3

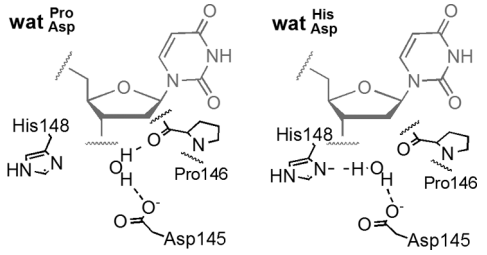

upper-bounds to the true ONIOM(MPWB1K/6-31G(d):PM3) barrier. Coordinates for all relaxed stationary points are provided in the Supporting Information. All calculations were carried out with Gaussian 09.[47]

RESULTS

To ensure that all options for water activation were investigated, models corresponding to chemically relevant orientations of the nucleophilic water molecule interacting with any residue within hydrogen-bonding distance were generated. Careful consideration of these active-site models led to reaction potential energy surfaces for three models, which encompass two water nucleophile orientations (Scheme 3) and two His148 protonation states. In the first (wat^{Pro}_{Asp}) model, the nucleophile is involved in hydrogen bonds with the functional group of Asp145 and the backbone carbonyl of Pro146. In the second model ($wat^{Pro}_{Asp}(+)$), the nucleophile orientation is the same as in wat^{Pro}_{Asp}, but His148 is protonated for comparison to previous computational work,[23] which adds an $N_\delta-H\cdots O$ hydrogen bond between His148 and the water nucleophile. Finally, in the wat^{His}_{Asp} model, the nucleophile acts as a proton donor to both His148 and Asp145.

The reaction potential energy surfaces corresponding to the three nucleophile models are presented in Figure 1. In the graphs, the reactant complex occurs on the left and the product complex on the right. Therefore, a dissociative mechanism will progress along the bottom of the plot, while an associative mechanism will occur near the top of the plot. A table of energies corresponding to each surface can be found in the Supporting Information (Tables S2−S4). In the following sections, each model will be described individually, and subsequently, results from point mutations on the most viable models will be presented.

The wat^{Pro}_{Asp} Model. In the wat^{Pro}_{Asp} model, the nucleophilic water molecule acts as a hydrogen donor to both the carboxylate group of Asp145 and the backbone carbonyl of Pro146 (Scheme 3). On the constrained PES (Figure 1A), the reactant occurs at a glycosidic bond length of 1.500 Å and a nucleophile distance of 3.000 Å. A transition state (TS) with a barrier of 25.4 kJ mol^{-1} (Table 1) can be identified with C1′−N1 and C1′−O_{nuc} distances of 2.100 and 2.600 Å, respectively. The TS is highly dissociative and slowly falls to an exothermic product (−24.7 kJ mol^{-1}, relative to the reactant) with a C1′−N1 distance of 3.300 Å and a C1′−O_{nuc} distance of 1.400 Å.

The relaxed stationary points for this mechanism have reaction coordinate distances similar to the constrained geometries (Figure 2 and Table S5). Furthermore, removing the constraints only slightly increases the barrier to 26.7 kJ mol^{-1} (Table 1). In the relaxed transition state (TS, Figure 2), the sugar moiety is nearly planar, which reflects oxacarbenium cation character. The

Table 1. Barrier Heights and Reaction Energies for the Mechanism of hUNG2 Action[a]

	constrained[b]		relaxed[c]	
model	$\Delta E^{\ddagger}$	ΔE_R	$\Delta E^{\ddagger}$	ΔE_R
wat^{Pro}_{Asp}	25.4	−24.7	26.7	−25.2
$wat^{Pro}_{Asp}(+)$	97.0	59.0	–[d]	–[d]
wat^{His}_{Asp}	32.8	−56.1	34.8	−57.8

[a] Energies (kJ mol^{-1}) calculated at the ONIOM(MPWB1K/6-31G(d):PM3) level of theory. [b] From constrained potential energy surfaces (see Figure 1). [c] From fully optimized stationary points. [d] Not determined (see text).

planar sugar, combined with a relatively large C1′−O_{nuc} distance (2.727 Å), indicates that this mechanism is dissociative in nature. In addition, attack of the water at C1′ is delayed with respect to dissociation of the nucleobase, where the hydrogen-bond distance between the nucleophile and the general base, Asp145, is large (2.176 Å) in the transition state. A tightening of the $N_\varepsilon-H\cdots O2$ hydrogen bond with His268 from 1.950 Å in the reactant to 1.880 Å in the transition state is observed in the relaxed complexes (Figure 2), which stabilizes the formation of the uracilate anion. The electrophilic C1′ migrates 0.793 Å toward the water nucleophile between the reactant and product complex, where the majority of this motion occurs after the transition state.

Throughout the reaction, Phe158 (Scheme 2) remains in a near parallel ($\pi-\pi$ stacked) orientation with respect to the uracil moiety, with an inter-ring distance of ∼4.1 Å. The phenyl ring is positioned above C4/N3 of uracil in the (relaxed) reactant and TS geometries but is centered over the pyrimidine ring in the product. The $N3-H\cdots O_\delta$ hydrogen bond to Asn204 increases from 1.839 to 1.851 Å between the reactant and product complexes, respectively. The $N_\delta-H\cdots O4$ interaction between Asn204 and uracil compresses by 0.013 Å in the transition state before returning to a length of 1.917 Å in the product. Finally, the hydrogen bond between a water molecule and O4 of uracil is reduced from 1.949 Å in the reactant to 1.925 Å in the TS and 1.889 Å in the product complex.

The $wat^{Pro}_{Asp}(+)$ Model. The $wat^{Pro}_{Asp}(+)$ model has the same nucleophile orientation as wat^{Pro}_{Asp}, but His148 is protonated at N_δ (Scheme 3). In the (constrained) reactant, His148 interacts with the nucleophile via a tight (1.705 Å) $N_\delta-H\cdots O_{nuc}$ hydrogen bond. This contact greatly reduces the nucleophilicity of the water molecule and results in a large barrier (97.0 kJ mol^{-1}) for addition to C1′ (Figure 1B, Table 2). Furthermore, the C1′−O_{nuc} distance in the transition state is very short (1.800 Å), which is in contrast to experimental evidence suggesting a highly dissociative reaction pathway. Therefore, it is very unlikely that the reaction will proceed with a cationic His148 residue, and this reaction will not be further refined through stationary point relaxation.

The wat^{His}_{Asp} Model. The final model employed in this study bridges the nucleophilic water between His148 and Asp145 (wat^{His}_{Asp}, Scheme 3). This water orientation has been previously proposed, based on a crystal structure of hUNG2 bound to an intermediate mimic.[14] The surface generated with this model (Figure 1C) is very similar in appearance to the wat^{Pro}_{Asp} PES (Figure 1A). The constrained reactant complex has glycosidic and nucleophilic distances of 1.500 and 3.600 Å, respectively. A TS can be observed at a C1′−N1 distance of 2.100 Å and a

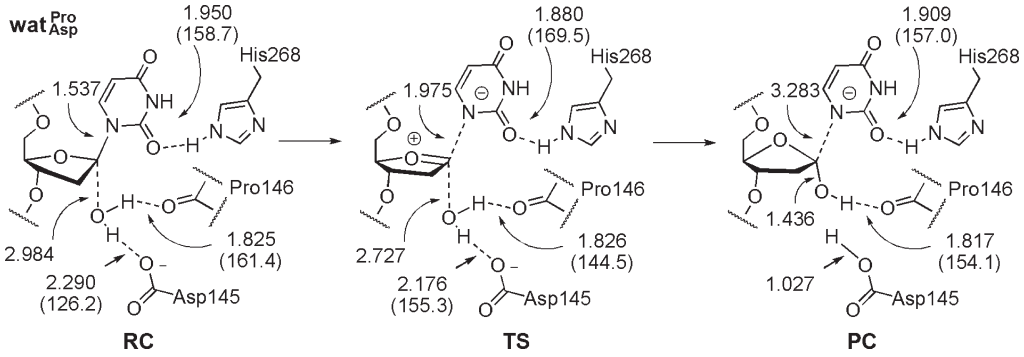

Figure 2. Important distances (Å) and angles (deg, in parentheses) for the relaxed stationary points from the wat^{Pro}_{Asp} model in which Asp145 is the general base and His148 neutral (ONIOM(MPWB1K/6-31G(d):PM3) optimized geometries).

Table 2. Changes in Calculated Barrier Heights Due to Single Mutations[a]

mutation	wat^{Pro}_{Asp}	wat^{His}_{Asp}	mutation	wat^{Pro}_{Asp}	wat^{His}_{Asp}
Asp145Asn	32.8	8.3	Gln144Gly	0.6	−2.8
His148Leu	7.6	7.0	Asp145Gly	19.2	12.1
Asn204Val	2.3	7.1	His148Gly	5.5	15.7
His268Ala	18.6	13.1	Phe158Gly	−1.8	−0.2
His268Leu	15.5	12.3	Asn204Gly	−[b]	7.2
His268Gln	5.2	6.8	His268Gly	18.7	13.2
			water[c]	7.1	6.9

[a] Relative energies (kJ mol^{-1}) calculated at the ONIOM(MPWB1K/6-31G(d):PM3) level of theory, where a positive value represents an increase in barrier height. [b] A stable structure could not be found. [c] Water molecule hydrogen bound at O4 of uracil was removed.

nucleophile distance of 3.200 Å and leads to an activation energy of 32.8 kJ mol^{-1}. This is close to the wat^{Pro}_{Asp} transition state in both geometry and energy (Table 1 and Table S5). After the TS, the surface steps down to an exothermic product (−56.1 kJ mol^{-1} relative to the reactant), which is significantly more stable than that on the wat^{Pro}_{Asp} surface. Interestingly, while this model allows for transfer to either Asp145 or His148 and thus does not explicitly bias nucleophile activation, proton transfer occurs from the nucleophile to His148 rather than Asp145.

There is very little change in geometry after releasing the reaction coordinate constraints on the reactant and transition state complexes. Therefore, when the constraints are removed from the wat^{His}_{Asp} stationary points, the barrier increases only slightly (to 34.8 kJ mol^{-1}). A notable difference upon full optimization is an increase in the C1′−N1 distance from 3.900 to 4.261 Å in the product (Table S5); however, there is only a very small change in the reaction energy (ΔE_R = −57.8 kJ mol^{-1}). Similar to the electrophile migration observed with the wat^{Pro}_{Asp} model, C1′ drifts 1.325 Å during the reaction, and the sugar moiety adopts a C1′-exo pucker at the end of the reaction.

The N_ε−H···O2 hydrogen bond between His268 and uracil reduces from 1.965 Å in the reactant to 1.876 Å in the transition state. In contrast to the wat^{Pro}_{Asp} model, the interplanar distance between the uracil group and Phe158 decreases from ∼4.1 to ∼3.6 Å as the reaction proceeds. This is accompanied by tightening of the hydrogen bonds to O2 and O4 of the uracilate anion. For example, the O−H···O4 interaction between an active-site water molecule and uracil reduces from 1.967 Å in the reactant to 1.892 Å in the product. Similarly, the N−H···O4 interaction with Asn204 decreases by 0.080 Å, and the N3−H···O_δ distance decreases from 2.015 to 1.844 Å from reactant to product. In addition, the N−H···O2 hydrogen bond between O2 of uracil and the backbone amine of Gln144 significantly shortens from 2.265 Å in the reactant to 1.981 and 1.788 Å in the transition state and product, respectively.

Point Mutations. Mutations involving Asp145, His148, Asn204, and His268 were performed on the two viable models (wat^{Pro}_{Asp} and wat^{His}_{Asp}) to allow for comparison of calculated (Table 2) and experimental[10,19] changes in the barrier height. The mutations were carried out on the constrained PES geometries to ensure that the transition state did not collapse to a minimum (reactant or product) when an essential residue was removed. The new R-group was positioned to have maximum overlap with the original R-group, this residue was optimized, and then the entire DFT region was relaxed (with the exception of the C1′−N1 and C1′−O_{nuc} constraints). While it is understood that the complex may rearrange in experimental studies to fill the vacancy created by mutations, our approach allows us to investigate the energetic (rather than structural) contribution of the mutations. We find the largest increase in barrier height (32.8 kJ mol^{-1}) for the Asp145Asn mutant with the wat^{Pro}_{Asp} model, which is partially due to a steric conflict between Asn145 and Gln144 (Scheme 2). Otherwise, the largest effects are seen for the His268Ala and His268Leu mutations, which are likely the result of the loss of the N_ε−H···O2 hydrogen bond.

The contributions of various residues (Gln144, Asp145, His148, Phe158, Asn204, and His268) to the calculated dissociation barrier were determined by replacing individual R groups with a hydrogen atom (i.e., mutation to glycine) (Table 2). Removing the residue that acts as the general base from each model leads to significant changes in barrier height. Specifically, removing Asp145 from the wat^{Pro}_{Asp} model increases the barrier by 19.2 kJ mol^{-1}. Similarly, a 15.7 kJ mol^{-1} contribution of His148 is calculated for the wat^{His}_{Asp} model. In addition, Asp145 lowers the wat^{His}_{Asp} barrier by 12.1 kJ mol^{-1}, which is similar to the contribution from the general base (His148). Two other groups yield large changes in the calculated activation energy. First, His268 contributes substantially to the catalytic effect of hUNG2, lowering the wat^{Pro}_{Asp} barrier by 18.7 kJ mol^{-1} and the wat^{His}_{Asp} barrier by 13.2 kJ mol^{-1}. Second, the water molecule hydrogen bound to O4 of uracil contributes nearly 7 kJ mol^{-1} to both the wat^{Pro}_{Asp} and wat^{His}_{Asp} barriers (Table 2), where the effect of this water molecule was ascertained through deletion of the entire molecule. No other significant changes to the barrier height were calculated with either model for any other mutation considered (Table 2).

dx.doi.org/10.1021/bi2003394 |*Biochemistry* 2011, 50, 4218–4227

DISCUSSION

His148 Not Cationic during Early Stages of Reaction. The mechanism of human uracil−DNA glycosylase action was examined with different water nucleophile interactions to thoroughly characterize both the uracil dissociation and water activation aspects of the reaction. While models containing a neutral His148 yield an activation energy (~30 kJ mol^{-1}) appropriate for enzyme catalysis, the reaction potential energy surface for the model with protonated His148 produces a comparatively large barrier (~100 kJ mol^{-1}, Table 1). This finding supports experimental evidence that His148 is neutral as the nucleobase dissociates[18] but contradicts a previous QM/MM study on hUNG2 that characterized a (~60 kJ mol^{-1}) barrier consistent with enzyme catalysis when His148 is protonated.[23] We suspected the discrepancy in the two computational studies is due to different partitioning schemes between the high- and low-level regions, where our model treats more active-site residues at the high (QM) level of theory. Therefore, single-point calculations were carried out on our $wat^{Pro}_{Asp}(+)$ geometries with the high-level region defined as in previous work (Figure S1A). These calculations yield an overall reaction pathway and energetics similar to those previously reported, which indicates that the earlier results were most likely obtained due to the use of a high-level region too small to properly describe the reaction. Furthermore, our large barrier calculated in the presence of a cationic His148 is more consistent with an anticipated decrease in the nucleophilicity of the water molecule upon protonation of this residue as well as an increase in electrostatic repulsion between cationic His148 and the positive charge developing on the sugar moiety. Since our model predicts a high barrier when His148 is protonated, and experimental evidence suggests this residue is neutral in the reactant,[18] only the wat^{Pro}_{Asp} and wat^{His}_{Asp} models will be discussed further.

Point Mutations Compare Well to Experiment. The experimental trend in activity for a selection of mutant enzymes (His148Leu > Asn204Val > His268Leu > Asp145Asn)[10] is predicted by both models containing neutral His148 (Table 2), within the error of our methodology. With respect to specific residues, the calculated effect of His268 on both models (Table 2) is consistent with the experimentally predicted contribution of this residue (9 − 20 kJ mol^{-1}).[7,17,20] Furthermore, the relatively small calculated effect (7.0−7.6 kJ mol^{-1}) of a His148Leu mutation on both barriers is in line with mutational analysis reporting an 8 kJ mol^{-1} effect on the barrier.[18] Most importantly, the calculated catalytic contribution of the previously proposed general base, Asp145, was found to be 19.2 and 12.1 kJ mol^{-1} for the wat^{Pro}_{Asp} and wat^{His}_{Asp} models, respectively. This is remarkably similar to the proposed transition state stabilization provided by Asp145 (12 kJ mol^{-1}) determined using intermediate mimics.[20]

Nucleotide Conformation Contributes to Catalysis. As mentioned in the Computational Details section, all hUNG2 active-site models were generated from a crystal structure (PDB ID: 1EMH) of the enzyme bound to DNA containing pseudouridine (ψU).[13] In this starting structure, C1 of ψU is bent ~40° from planarity toward an sp^3-hybridized geometry. When ψU is mutated to uracil to generate the reactant geometries, the bend is greatly reduced (<20°) but does not entirely disappear. Optimization of the nucleoside configuration found in the current work with no enzyme present removes the bend at N1 of uracil, which eliminates the possibility that the kink is an artifact of the DFT method implemented. In addition, the χ dihedral angle about the glycosidic bond in the relaxed enzyme-bound deoxyuridine reactant (170°−180°) deviates by ~40° from the free nucleoside optimized at the same level of theory. Thus, both geometric features are likely due to steric constraints in the active site (Scheme 2), particularly the close proximity of Phe158, as well as strong hydrogen-bonding interactions with Asn204 and His268.[21,48] Although the altered conformation of the reactant was originally reported for a substrate mimic (ψU),[13] our calculations show that these deformations persist with 2′-deoxyuridine. As suggested in previous work, these geometrical changes to the dU nucleotide likely have a significant contribution to the catalytic effect of hUNG2 by lowering the barrier to deglycosylation through hyperconjugation and anomeric effects.[13,48] We calculate that this change in conformation requires over 10 kJ mol^{-1}.[b] Therefore, while the activation energies calculated using our two viable models (26.7 and 34.8 kJ mol^{-1}, for wat^{Pro}_{Asp} and wat^{His}_{Asp}, respectively) are lower than the experimental value (50.6 kJ mol^{-1}),[49,50] at least some of this difference can be attributed to bending of the nucleotide to fit into the active site.

hUNG2 Mechanism Highly Dissociative. Calculations on both of our viable models suggest that the reaction has a single transition state that is highly dissociative in nature. Specifically, the transition state for both the wat^{Pro}_{Asp} and wat^{His}_{Asp} models exhibits a glycosidic bond length of ~2 Å and a considerably longer nucleophile distance (>2.6 Å). After the transition state, the potential energy surface has a flat plateau corresponding to further stretching of the glycosidic bond. Once the glycosidic bond is sufficiently elongated, C1′ electrophile migration toward the water nucleophile and barrierless addition of water to the anomeric carbon occurs. While it has been proposed that a stable intermediate exists along the reaction pathway, our calculations support a transition state that is highly dissociative and has substantial oxacarbenium ion character as suggested by KIE experiments.[8] In addition, the shape of our calculated PES following the transition state is supported by evidence that nucleophilic addition to oxacarbenium cations is often barrierless.[51,52] Regardless, our models indicate that the nucleophile is deprotonated before, rather than after, addition to the anomeric carbon, and therefore nucleophile activation likely plays a role in the barrierless addition in this particular reaction. Taken together, the comparisons in the above paragraphs support the use of both the wat^{Pro}_{Asp} and wat^{His}_{Asp} active-site models and allows us to examine other aspects of the chemical step of the hUNG2 mechanism with confidence.

Active-Site Residues Trade-Off Stabilizing Negative Charge Forming on Uracil. A benefit to carrying out reaction PES scans is the ability to observe how substrate interactions change during the course of the reaction, which in turn permits predictions about the role of active-site residues. Our most important finding from this analysis is that several amino acid residues share the responsibility of stabilizing the negative charge building up on the uracil moiety throughout the reaction despite emphasis on only His268 in the literature. Furthermore, each group provides stabilization at slightly different stages of the reaction. The interactions involving O4 of uracil are at their strongest earlier in the reaction (C1′−N1 = 2.1−2.5 Å) since this site has the largest proton affinity in the neutral nucleobase.[53] Specifically, the hydrogen bond between Asn204 and O4 of the uracil moiety is shortest immediately following the TS (Table S7). The interactions involving O2 are strongest later in the reaction since the negative charge in the uracilate anion is

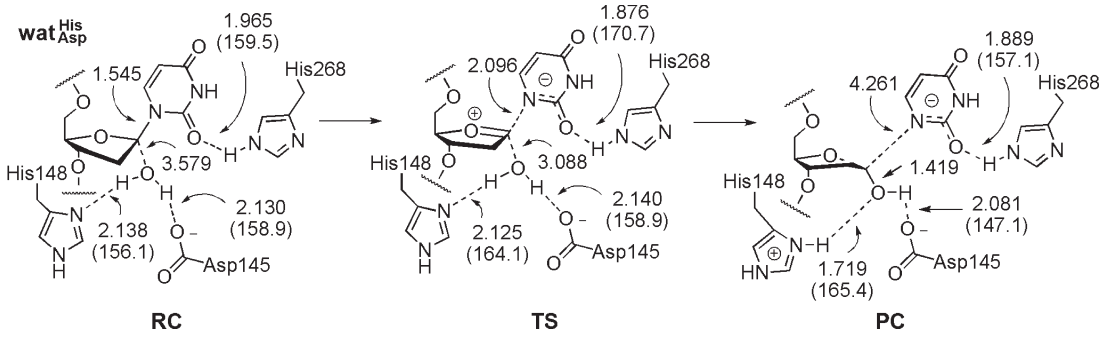

Figure 3. Important distances (Å) and angles (deg, in parentheses) for the relaxed stationary points from the wat^{His}_{Asp} model in which His148 is the general base (ONIOM(MPWB1K/6-31G(d):PM3) optimized geometries).

delocalized over N1/O2. Indeed, the interaction between the catalytic His268 residue and O2 is strongest when the C1′−N1 distance is around 2.7−2.9 Å. Interestingly, interactions between O4 and an active-site water molecule also change during the reaction, where these interactions are strongest just before the product complex. These effects are observed for both the wat^{Pro}_{Asp} and wat^{His}_{Asp} models; however, the changes in hydrogen-bond length throughout the reaction are more pronounced for the wat^{His}_{Asp} model (see Supporting Information, Table S7). For both models, changes in the interactions between uracil and any other active-site amino acid residues are insignificant.

Asp145 Mutations Can Mask Effects of Residues Important Later in the Chemical Step. As mentioned in the Results section, the Asp145Gly mutation to both the wat^{Pro}_{Asp} and wat^{His}_{Asp} models leads to a significant change in barrier height (19.2 and 12.1 kJ mol^{-1}, respectively, Table 2). Since the TS is highly dissociative, this is consistent with suggestions that Asp145 electrostatically stabilizes the sugar moiety in the TS.[20,26] Furthermore, since association of the water nucleophile is barrierless (Figure 1), mutations that remove Asp145 can conceal the effects of residues on processes that occur later along the reaction pathway, such as the role of His148 in activation of the nucleophile. For example, the His148Leu effect on the barrier for both models is ∼7.0 kJ mol^{-1} (Table 2), which indicates a smaller dependence of the dissociative TS on this residue, despite being the general base in one of the models. This suggests that the contribution of His148 occurs after the rate-limiting step and therefore may not be observed in mutations (e.g., Asp145Asn) that disrupt dissociation of the nucleobase. On the basis of this discussion, it may not be possible to conclusively determine the role of Asp145 as the general base or the role of other residues (i.e., His148) in the chemical step of the hUNG2 mechanism following base departure by point mutations alone.

His148 Is Preferred over Asp145 as the General Base. Deletion of the acting general base from either the wat^{Pro}_{Asp} or wat^{His}_{Asp} models (Asp145 and His148, respectively) causes the nucleophile to reorient to interact with the other potential activator. Therefore, in the absence of His148, Asp145 can act as the general base and vice versa. When coupled with similar calculated reaction barriers (26.7 and 34.8 kJ mol^{-1}, Table 2), this finding suggests that either Asp145 or His148 may activate the water nucleophile depending on the orientation the water is bound in the active site. However, the preference for proton transfer from the nucleophile to one base over the other can be ascertained by examining the wat^{His}_{Asp} model, which allows for water activation by either His148 or Asp145. In the relaxed wat^{His}_{Asp} reactant complex (RC, Figure 3), the hydrogen-bond distances between the nucleophile and the two potential general bases (His148 and Asp145) are almost identical. Nevertheless, the contact to His148 tightens and that to Asp145 loosens in the transition state. In addition, the nucleophilic water fully transfers a proton to His148 in the product complex, which contrasts the incomplete transfer in the wat^{Pro}_{Asp} product (PC, Figure 2). This demonstrates that proton transfer to histidine is preferred, which is consistent with proposals that hydrogen bonds formed between groups with matching pK_a's can provide a large contribution to enzyme catalysis[54] since the pK_a of water is closer to histidine than aspartate. Therefore, while either Asp145 or His148 can act as the general base in the mechanism of hUNG2 action, our calculations indicate that proton transfer to histidine is more likely.

Roles of Asp145 and His148. Our calculations suggest that both Asp145 and His148 are required for maximum efficiency of the chemical step. During the early stages of the reaction, the water nucleophile is held in place by an anionic Asp145 and a neutral His148, which confirms this previously hypothesized function of His148.[18] However, we further expand the role of His148 to include activation of the nucleophile (i.e., catalyzes AP-site formation). This newly proposed function is supported by the work of Parker and Stivers,[18] who found that His148 is initially neutral, but becomes protonated during the reaction, and has a catalytic contribution late in the chemical step. Furthermore, they proposed that His148 should be added to the list of important active-site groups for transition state stabilization, potentially through positioning the substrate and catalytic water or producing a favorable reaction environment (solvent exclusion). We agree that His148 is an important catalytic residue and reveal for the first time that its primary role in the chemical step is likely activation of the water nucleophile. We note that this new function for His148 does not exclude possible significant contributions to earlier events such as nucleotide flipping or active-site reorganization.[18,28] Finally, in agreement with previous proposals,[20] we assign the primary role of Asp145 to electrostatic stabilization of the cationic sugar moiety formed as the reaction proceeds (i.e., catalyzes glycosidic bond cleavage). Recently, it has been proposed that the role of the catalytically essential lysine in hOGG1 as the nucleophile is secondary to its role in substrate recognition and binding and is the direct result of its proximity to the sugar.[55] When this concept is applied to Asp145 in hUNG2, the proximity of the Asp145 residue to the water nucleophile resulting from its primary role of electrostatic stabilization of the TS allows participation in proton transfer as a possible secondary role. Prioritizing the functions of Asp145 in this manner aligns

the role of this residue in hUNG2 with the accepted primary function of active-site aspartate or glutamate residues similarly positioned in other glycosylases.[4,5,29−32,34]

CONCLUSIONS

In the present work, ONIOM(QM:QM) calculations were utilized to study the reaction potential energy surfaces of the mechanism of hUNG2 action. Unlike previous computational work that treated fewer active-site residues with a high (QM) level of theory, we determined that His148 must be neutral during dissociation of the nucleobase, which is consistent with recent experimental evidence. The reaction potential energy surfaces generated using two models with neutral His148 residues are both consistent with an abundance of experimental data, including mutational studies. This supports the use of our active-site models and allows us to confidently examine different aspects of the chemical step catalyzed by hUNG2.

For the first time, we present a complete mechanism for the chemical step of hUNG2 action where His268, Asp145, *and* His148 are catalytic. Specifically, in agreement with previous literature, we propose that the primary function of Asp145 is electrostatic stabilization of the cationic charge forming on the sugar moiety. Therefore, this residue catalyzes glycosidic bond cleavage in conjunction with His268. Although this role for His268 has been previously proposed, we demonstrate that Asn204 and a water molecule are also involved in stabilization of the negative charge on uracil, where the importance of these interactions changes throughout the course of the reaction. In addition, while we find that Asp145 can act as the general base, we reveal for the first time that His148 preferentially activates the water nucleophile in the chemical step. By classifying water activation, as well as nucleophile orientation, as a potential secondary function of Asp145, the primary (electrostatic stabilization) role of this residue becomes aligned with that of active-site carboxylate groups in other glycosylases. Most importantly, our work supports the incorporation of His148 into the list of residues (Asp145 and His268) essential to the chemical step of the hUNG2 mechanism and explains the experimental observation that this residue contributes to the catalysis of the chemical step.

ASSOCIATED CONTENT

Supporting Information. Definitions of the active-site model and high-level region, tables of energies for PES plots, comparison of distances between constrained and relaxed geometries, bar graph of the mutational effects, tables of important contact distances, and optimized coordinates for all relaxed geometries. This material is available free of charge via the Internet at http://pubs.acs.org.

AUTHOR INFORMATION

Corresponding Author

*E-mail: stacey.wetmore@uleth.ca. Phone: 403-329-2323. Fax: 403-329-2057.

Funding Sources

This research was supported by the Natural Sciences and Engineering Research Council (NSERC), the Canada Research Chair program and the Canada Foundation for Innovation (CFI) for S.D.W., and an NSERC graduate student scholarship (CGS-D) for J.L.P. Calculations were conducted on the Up-scale and Robust Abacus for Chemistry in Lethbridge (URACIL) computing cluster.

ABBREVIATIONS

AP-site, apyrimidinic site; DFT, density functional theory; eUDG, *Escherichia coli* uracil−DNA glycosylase; hOGG1, human 8-oxoguanine DNA glycosylase; hUNG2, human uracil−DNA glycosylase; MM, molecular mechanics; MPWB1K, modified Perdew−Wang 91 exchange with Becke 95 correlation functional; ONIOM, our own N-layered integrated molecular orbital; ψU, pseudouridine; PES, potential energy surface; PM3, Parameterized Model 3; QM, quantum mechanics; QST, quadratic synchronous transit method; TS, transition state; wat^{His}_{Asp}, His148 modeled as general base; wat^{Pro}_{Asp}, Asp145 modeled as general base with neutral His148; $wat^{Pro}_{Asp}(+)$, Asp145 modeled as general base with cationic His148.

ADDITIONAL NOTE

[a] Human uracil−DNA glycosylase numbering will be used throughout.

[b] Calculated at the MPWB1K/6-31G(d) level of theory by fixing the N1 out-of-plane angle in the bare dU nucleoside in the gas phase.

REFERENCES

(1) Lindahl, T. (1974)An N-Glycosidase from *Eschirichia coli* that Releases Free Uracil from DNA Containing Deaminated Cytosine Residues. *Proc. Natl. Acad. Sci. U.S.A. 71*, 3649–3653.

(2) Krokan, H., and Wittwer, C. U. (1981)Uracil DNA-Glycosylase from HeLa-Cells - General-Properties, Substrate-Specificity and Effect of Uracil Analogs. *Nucleic Acids Res. 9*, 2599–2613.

(3) Kavli, B., Sundheim, O., Akbari, M., Otterlei, M., Nilsen, H., Skorpen, F., Aas, P. A., Hagen, L., Krokan, H. E., and Slupphaug, G. (2002)hUNG2 is the Major Repair Enzyme for Removal of Uracil from U:A Matches, U:G Mismatches, and U in Single-Stranded DNA, with hSMUG1 as a Broad Specificity Backup. *J. Biol. Chem. 277*, 39926–39936.

(4) Blackburn, G. M., and Walcher, G. (2001)No Strain, No Gain": Studies in the Mechanism of a DNA Repair Enzyme. *Pol. J. Chem. 75*, 1183–1194.

(5) Stivers, J. T., and Jiang, Y. L. (2003)A Mechanistic Perspective on the Chemistry of DNA Repair Glycosylases. *Chem. Rev. (Washington, DC, U. S.) 103*, 2729–2759.

(6) Berti, P. J., and McCann, J. A. B. (2006)Toward a Detailed Understanding of Base Excision Repair Enzymes: Transition State and Mechanistic Analyses of N-glycoside Hydrolysis and N-glycoside Transfer. *Chem. Rev. (Washington, DC, U. S.) 106*, 506–555.

(7) Dong, J., Drohat, A. C., Stivers, J. T., Pankiewicz, K. W., and Carey, P. R. (2000)Raman Spectroscopy of Uracil DNA Glycosylase-DNA Complexes: Insights into DNA Damage Recognition and Catalysis. *Biochemistry 39*, 13241–13250.

(8) Werner, R. M., and Stivers, J. T. (2000)Kinetic Isotope Effect Studies of the Reaction Catalyzed by Uracil DNA Glycosylase: Evidence for an Oxocarbenium Ion-Uracil Anion Intermediate. *Biochemistry 39*, 14054–14064.

(9) Mol, C. D., Arvai, A. S., Sanderson, R. J., Slupphaug, G., Kavli, B., Krokan, H. E., Mosbaugh, D. W., and Tainer, J. A. (1995)Crystal Structure of Human Uracil-DNA Glycosylase in Complex with a Protein Inhibitor: Protein Mimicry of DNA. *Cell (Cambridge, MA, U. S.) 82*, 701–708.

(10) Mol, C. D., Arvai, A. S., Slupphaug, G., Kavli, B., Alseth, I., Krokan, H. E., and Tainer, J. A. (1995)Crystal Structure and Mutational

Analysis of Human Uracil-DNA Glycosylase: Structural Basis of Specificity and Catalysis. *Cell (Cambridge, MA, U. S.) 80*, 869–878.

(11) Slupphaug, G., Mol, C. D., Kavli, B., Arvai, A. S., Krokan, H. E., and Tainer, J. A. (1996)A Nucleotide-Flipping Mechanism from the Structure of Human Uracil-DNA Glycosylase Bound to DNA. *Nature (London, U. K.) 384*, 87–92.

(12) Parikh, S. S., Mol, C. D., Slupphaug, G., Bharati, S., Krokan, H. E., and Tainer, J. A. (1998)Base Excision Repair Initiation Revealed by Crystal Structures and Binding Kinetics of Human Uracil-DNA Glycosylase with DNA. *EMBO J. 17*, 5214–5226.

(13) Parikh, S. S., Walcher, G., Jones, G. D., Slupphaug, G., Krokan, H. E., Blackburn, G. M., and Tainer, J. A. (2000)Uracil-DNA Glycosylase-DNA Substrate and Product Structures: Conformational Strain Promotes Catalytic Efficiency by Coupled Stereoelectronic Effects. *Proc. Natl. Acad. Sci. U.S.A. 97*, 5083–5088.

(14) Bianchet, M. A., Seiple, L. A., Jiang, Y. L., Ichikawa, Y., Amzel, L. M., and Stivers, J. T. (2003)Electrostatic Guidance of Glycosyl Cation Migration Along the Reaction Coordinate of Uracil DNA Glycosylase. *Biochemistry 42*, 12455–12460.

(15) Drohat, A. C., Xiao, G. Y., Tordova, M., Jagadeesh, J., Pankiewicz, K. W., Watanabe, K. A., Gilliland, G. L., and Stivers, J. T. (1999) Heteronuclear NMR and Crystallographic Studies of Wild-Type and H187Q *Escherichia coli* Uracil DNA Glycosylase: Electrophilic Catalysis of Uracil Expulsion by a Neutral Histidine 187. *Biochemistry 38*, 11876–11886.

(16) Drohat, A. C., and Stivers, J. T. (2000)*Escherichia coli* Uracil DNA Glycosylase: NMR Characterization of the Short Hydrogen Bond from His187 to Uracil O2. *Biochemistry 39*, 11865–11875.

(17) Drohat, A. C., and Stivers, J. T. (2000)NMR Evidence for an Unusually Low N1 pK(a) for Uracil Bound to Uracil DNA Glycosylase: Implications for Catalysis. *J. Am. Chem. Soc. 122*, 1840–1841.

(18) Parker, J. B., and Stivers, J. T. (2008)Uracil DNA Glycosylase: Revisiting Substrate-Assisted Catalysis by DNA Phosphate Anions. *Biochemistry 47*, 8614–8622.

(19) Drohat, A. C., Jagadeesh, J., Ferguson, E., and Stivers, J. T. (1999)Role of Electrophilic and General Base Catalysis in the Mechanism of *Escherichia coli* Uracil DNA Glycosylase. *Biochemistry 38*, 11866–11875.

(20) Jiang, Y. L., Drohat, A. C., Ichikawa, Y., and Stivers, J. T. (2002) Probing the Limits of Electrostatic Catalysis by Uracil DNA Glycosylase Using Transition State Mimicry and Mutagenesis. *J. Biol. Chem. 277*, 15385–15392.

(21) Shaw, R. W., Feller, J. A., and Bloom, L. B. (2004)Contribution of a Conserved Phenylalanine Residue to the Activity of *Escherichia coli* Uracil DNA Glycosylase. *DNA Repair 3*, 1273–1283.

(22) Luo, N., Mehler, E., and Osman, R. (1999)Specificity and Catalysis of Uracil DNA Glycosylase. A Molecular Dynamics Study of Reactant and Product Complexes with DNA. *Biochemistry 38*, 9209–9220.

(23) Dinner, A. R., Blackburn, G. M., and Karplus, M. (2001)Uracil-DNA Glycosylase Acts by Substrate Autocatalysis. *Nature (London, U. K.) 413*, 752–755.

(24) Ma, A., Hu, J., Karplus, M., and Dinner, A. R. (2006)Implications of Alternative Substrate Binding Modes for Catalysis by Uracil-DNA Glycosylase: An Apparent Discrepancy Resolved. *Biochemistry 45*, 13687–13696.

(25) Millen, A. L., Archibald, L. A. B., Hunter, K. C., and Wetmore, S. D. (2007)A Kinetic and Thermodynamic Study of the Glycosidic Bond Cleavage in Deoxyuridine. *J. Phys. Chem. B 111*, 3800–3812.

(26) Jiang, Y. L., Cao, C., Stivers, J. T., Song, F., and Ichikawa, Y. (2004)The Merits of Bipartite Transition-State Mimics for Inhibition of Uracil DNA Glycosylase. *Bioorg. Chem. 32*, 244–262.

(27) Wolfenden, R. (2006)Degrees of Difficulty of Water-Consuming Reactions in the Absence of Enzymes. *Chem. Rev. (Washington, DC, U. S.) 106*, 3379–3396.

(28) Parker, J. B., Bianchet, M. A., Krosky, D. J., Friedman, J. I., Amzel, L. M., and Stivers, J. T. (2007)Enzymatic Capture of an Extrahelical Thymine in the Search for Uracil in DNA. *Nature (London, U. K.) 449*, 433–438.

(29) Norman, D. P. G., Chung, S. J., and Verdine, G. L. (2003) Structural and Biochemical Exploration of a Critical Amino Acid in Human 8-oxoguanine Glycosylase. *Biochemistry 42*, 1564–1572.

(30) Fromme, J. C., and Verdine, G. L. (2003)DNA Lesion Recognition by the Bacterial Repair Enzyme MutM. *J. Biol. Chem. 278*, 51543–51548.

(31) Fromme, J. C., and Verdine, G. L. (2003)Structure of a Trapped Endonuclease III-DNA Covalent Intermediate. *EMBO J. 22*, 3461–3471.

(32) Doublie, S., Bandaru, V., Bond, J. P., and Wallace, S. S. (2004) The Crystal Structure of Human Endonuclease VIII-Like 1 (NEIL1) Reveals a Zincless Finger Motif Required for Glycosylase Activity. *Proc. Natl. Acad. Sci. U.S.A. 101*, 10284–10289.

(33) Lau, A. Y., Wyatt, M. D., Glassner, B. J., Samson, L. D., and Ellenberger, T. (2000)Molecular Basis for Discriminating Between Normal and Damaged Bases by the Human Alkyladenine Glycosylase, AAG. *Proc. Natl. Acad. Sci. U.S.A. 97*, 13573–13578.

(34) Fromme, J. C., Banerjee, A., Huang, S. J., and Verdine, G. L. (2004)Structural Basis for Removal of Adenine Mispaired with 8-Oxoguanine by MutY Adenine DNA Glycosylase. *Nature (London, U. K.) 427*, 652–656.

(35) Bowman, B. R., Lee, S., Wang, S. Y., and Verdine, G. L. (2010) Structure of *Escherichia coli* AlkA in Complex with Undamaged DNA. *J. Biol. Chem. 285*, 35783–35791.

(36) Humbel, S., Sieber, S., and Morokuma, K. (1996)The IMOMO Method: Integration of Different Levels of Molecular Orbital Approximations for Geometry Optimization of Large Systems: Test for n-Butane Conformation and S(N)2 Reaction: RCl+Cl. *J. Chem. Phys. 105*, 1959–1967.

(37) Dapprich, S., Komaromi, I., Byun, K. S., Morokuma, K., and Frisch, M. J. (1999)A New ONIOM Implementation in Gaussian98. Part I. The Calculation of Energies, Gradients, Vibrational Frequencies and Electric Field Derivatives. *THEOCHEM 462*, 1–21.

(38) Lundberg, M., Kawatsu, T., Vreven, T., Frisch, M. J., and Morokuma, K. (2009)Transition States in a Protein Environment-ONIOM QM:MM Modeling of Isopenicillin N Synthesis. *J. Chem. Theory Comput. 5*, 222–234.

(39) Stewart, J. J. P. (1989)Optimization of Parameters for Semiemperical Methods. 1. Method. *J. Comput. Chem. 10*, 209–220.

(40) Stewart, J. J. P. (1989)Optimizations of Parameters for Semiemperical Methods. 2. Applications. *J. Comput. Chem. 10*, 221–264.

(41) Zhao, Y., and Truhlar, D. G. (2004)Hybrid Meta Density Functional Theory Methods for Thermochemistry, Thermochemical Kinetics, and Noncovalent Interactions: The MPW1B95 and MPWB1K Models and Comparative Assessments for Hydrogen Bonding and Van der Waals Interactions. *J. Phys. Chem. A 108*, 6908–6918.

(42) Cisneros, G. A. s., Perera, L., Schaaper, R. M., Pedersen, L. C., London, R. E., Pedersen, L. G., and Darden, T. A. (2009)Reaction Mechanism of the ε Subunit of *E. coli* DNA Polymerase III: Insights into Active Site Metal Coordination and Catalytically Significant Residues. *J. Am. Chem. Soc. 131*, 1550–1556.

(43) Parks, J. M., Guo, H., Momany, C., Liang, L., Miller, S. M., Summers, A. O., and Smith, J. C. (2009)Mechanism of Hg-C Protonolysis in the Organomercurial Lyase MerB. *J. Am. Chem. Soc. 131*, 13278–13285.

(44) Tao, P., Gatti, D. L., and Schlegel, H. B. (2009)The Energy Landscape of 3-Deoxy-d-manno-octulosonate 8-Phosphate Synthase. *Biochemistry 48*, 11706–11714.

(45) Lonsdale, R., Harvey, J. N., and Mulholland, A. J. (2010) Compound I Reactivity Defines Alkene Oxidation Selectivity in Cytochrome P450cam. *J. Phys. Chem. B 114*, 1156–1162.

(46) Tao, P., Fisher, J. F., Shi, Q., Mobashery, S., and Schlegel, H. B. (2010)Matrix Metalloproteinase 2 (MMP2) Inhibition: DFT and QM/MM Studies of the Deprotonation-Initialized Ring-Opening Reaction of the Sulfoxide Analogue of SB-3CT. *J. Phys. Chem. B 114*, 1030–1037.

(47) Frisch, M. J., Trucks, G. W., Schlegel, H. B. Scuseria, G. E., Robb, M. A., Cheeseman, J. R., Scalmani, G., Barone, V., Mennucci, B., Petersson, G. A., Nakatsuji, H., Caricato, M., Li, X., Hratchian, H. P., Izmaylov, A. F., Bloino, J., Zheng, G., Sonnenberg, J. L., Hada, M., Ehara,

M., Toyota, K., Fukuda, R., Hasegawa, J., Ishida, M., Nakajima, T., Honda, Y., Kitao, O., Nakai, H., Vreven, T., Montgomery, Jr., J. A., Peralta, J. E., Ogliaro, F., Bearpark, M., Heyd, J. J., Brothers, E., Kudin, K. N., Staroverov, V. N., Kobayashi, R., Normand, J., Raghavachari, K., Rendell, A., Burant, J. C., Iyengar, S. S., Tomasi, J., Cossi, M., Rega, N., Millam, N. J., Klene, M., Knox, J. E., Cross, J. B., Bakken, V., Adamo, C., Jaramillo, J., Gomperts, R., Stratmann, R. E., Yazyev, O., Austin, A. J., Cammi, R., Pomelli, C., Ochterski, J. W., Martin, R. L., Morokuma, K., Zakrzewski, V. G., Voth, G. A., Salvador, P., Dannenberg, J. J., Dapprich, S., Daniels, A. D., Farkas, Ö., Foresman, J. B., Ortiz, J. V., Cioslowski, J., and Fox, D. J. (2009) *Gaussian 09*, Revision A.1, Gaussian, Inc., Wallingford, CT.

(48) Werner, R. M., Jiang, Y. L., Gordley, R. G., Jagadeesh, G. J., Ladner, J. E., Xiao, G. Y., Tordova, M., Gilliland, G. L., and Stivers, J. T. (2000)Stressing-Out DNA? The Contribution of Serine-Phosphodiester Interactions in Catalysis by Uracil DNA Glycosylase. *Biochemistry 39*, 12585–12594.

(49) Wittwer, C. U., and Krokan, H. (1985)Uracil-DNA Glycosylase in HeLa S3 Cells: Interconvertibility of 50 and 20 kDa Forms and Similarity of the Nuclear and Mitochondrial Form of the Enzyme. *Biochim. Biophys. Acta, Protein Struct. Mol. Enzymol. 832*, 308–318.

(50) Slupphaug, G., Eftedal, I., Kavli, B., Bharati, S., Helle, N. M., Haug, T., Levine, D. W., and Krokan, H. E. (1995)Properties of a Recombinant Human Uracil-DNA Glycosylase from the *Ung* Gene and Evidence That *Ung* Encodes the Major Uracil-DNA Glycosylase. *Biochemistry 34*, 128–138.

(51) Richard, J. P. (1995)A Consideration of the Barrier for Carbocation-Nucleophile Combination Reactions. *Tetrahedron 51*, 1535–1573.

(52) Richard, J. P., Williams, K. B., and Amyes, T. L. (1999)Intrinsic Barriers for the Reactions of an Oxocarbenium Ion in Water. *J. Am. Chem. Soc. 121*, 8403–8404.

(53) Di Laudo, M., Whittleton, S. R., and Wetmore, S. D. (2003) Effects of Hydrogen Bonding on the Acidity of Uracil. *J. Phys. Chem. A 107*, 10406–10413.

(54) Cleland, W. W., and Kreevoy, M. M. (1994)Low-Barrier Hydrogen-Bonds and Enzymatic Catalysis. *Science (Washington, DC, U. S.) 264*, 1887–1890.

(55) Dalhus, B., Forsbring, M., Helle, I. H., Vik, E. S., Forstrøm, R. J., Backe, P. H., Alseth, I., and Bjørås, M. (2011)Separation-of-Function Mutants Unravel the Dual-Reaction Mode of Human 8-Oxoguanine DNA Glycosylase. *Structure (Cambridge, MA, U. S.) 19*, 117–127.